INTERNATIONAL JOURNAL OF
NUMERICAL ANALYSIS AND MODELING
Volume 13, Number 2, Pages 244–264

LINEAR AND QUADRATIC FINITE VOLUME METHODS ON TRIANGULAR MESHES FOR ELLIPTIC EQUATIONS WITH SINGULAR SOLUTIONS

GUANGHAO JIN, HENGGUANG LI, QINGHUI ZHANG, AND QINGSONG ZOU

Abstract. This paper is devoted to the presentation and analysis of some linear and quadratic finite volume (FV) schemes for elliptic problems with singular solutions due to the non-smoothness of the domain. Our FV schemes are constructed over specially-designed graded triangular meshes. We provide sharp parameter selection criteria for the graded mesh, such that both the linear and quadratic FV schemes achieve the optimal convergence rate approximating singular solutions in H^1. In addition, we show that on the same mesh, a linear FV scheme obtains the optimal rate of convergence in L^2. Numerical tests are provided to verify the analysis.

Key words. Finite volume method, singular solution, optimal convergence rate.

1. Introduction

With good local flux-conservation properties, the finite volume method (FVM) is used in a wide range of computations, especially in computational fluid dynamics (see [5, 25, 28, 30, 39, 40, 41, 44] and references therein). The mathematical theory of FVM [19, 30, 34] has not been fully developed, at least, not as satisfactory as that for the finite element method. Most works concentrate on linear or quadratic schemes on quasi-uniform meshes (see e.g., [4, 7, 18, 23, 34, 35, 45]). In addition, a few studies have been conducted for high order FV schemes. We here mention 1D high order FV schemes [8, 42], high order FV schemes over rectangular meshes [6, 46], and high order FV schemes over triangular meshes [11, 12]. These high order methods are efficient when the solution of the problem is sufficiently smooth.

It is well known that the solution of elliptic equations may have singularities due to the non-smoothness of the domain, even when the other given data are smooth. In particular, consider the Poisson problem

$$-\Delta u = f \quad \text{in} \quad \Omega, \qquad u = 0 \quad \text{on} \quad \partial\Omega, \tag{1}$$

where Ω is a bounded polygonal domain in $\mathbb{R}^2$. Then, given $f \in H^{-1}(\Omega) = H_0^1(\Omega)'$, there exists a unique solution $u \in H_0^1(\Omega)$ to (1), defined by the variational form

$$a(u, v) = \int_\Omega \nabla u \cdot \nabla v dx = \int_\Omega f v dx, \qquad \forall\ v \in H_0^1(\Omega). \tag{2}$$

Received by the editors March 15, 2015.

2000 *Mathematics Subject Classification.* 65N08, 65N15, 65N50, 35J15.

H. Li was partially supported by the NSF Grants DMS-1158839, DMS-1418853, and the Wayne State University Grants Plus Program. Q. Zhang was partially supported by the Natural Science Foundation of China under grant 11001282 and 11471343, and Guangdong Provincial Natural Science Foundation of China under grant 2015A030306016. Q. Zou was partially supported by the National Natural Science Foundation of China through grants 11571384 and 11428103, and by Guangdong Provincial Natural Science Foundation of China under grant through grant 2014A030313179.

Correspondence to Qingsong Zou : mcszqs@mail.sysu.edu.cn.

In the case that the boundary $\partial\Omega$ is smooth, we have the *full regularity* estimate for the solution [17, 20, 36],

$$\|u\|_{H^{m+1}(\Omega)} \leq C\|f\|_{H^{m-1}(\Omega)}, \qquad m \geq 0, \tag{3}$$

where the constant $C > 0$ depends on the domain, but not on f. On a polygonal domain Ω, however, the full regularity result holds only in the interior region away from the vertices. On the entire domain Ω, the solution u may only belong to $H^{1+s}(\Omega)$ for a given smooth function f, where s is fixed and depends on the geometry of the boundary.

The singularity in the solution can significantly slow down the convergence rate of the numerical approximation, as well as raise concerns on the theoretical justification of the numerical scheme. Compared with the tremendous effort to develop optimal finite element algorithms [1, 2, 3, 22, 29, 33, 38, 43], fewer results are available on the FVMs for singular solution, and most of them only concern linear FV schemes. See [9, 15] and reference therein for some relevant works. In particular, three *linear* FVMs are proposed in [15] to approximate solutions of equation (1) with corner singularities. The mesh and dual mesh are carefully designed, such that the associated FV solutions achieve the optimal rate of convergence that is expected for smooth solutions.

In this paper, we develop new *linear* and *quadratic* FVMs approximating singular solutions of equation (1). In particular, we give a simple and explicit construction of graded meshes and the dual meshes, such that the associated linear and quadratic FV solutions achieve the optimal convergence rate in the H^1-norm. In addition, we will show that the L^2-convergence rate of the proposed linear FVM is also optimal. Our analysis is based on the stability of the FV schemes, sharp regularity estimates in suitable weighted Sobolev spaces, and rigorous interpolation error estimates in these spaces. These results extend to more general elliptic equations. It is also possible to apply the analytical tools developed here to other high order well-posed FVMs.

The rest of the paper is organized as follows. In Section 2, we introduce the linear and quadratic FV schemes and the graded triangular meshes. Determined by a set of grading parameters, these graded meshes have good geometric properties that will also be discussed. In Section 3, we present the detailed analysis in suitable function spaces and obtain the main result of the paper. In particular, we give regularity estimates, interpolation error estimates, and the continuity estimates of the FV bilinear forms. Using these results, in Theorem 3.9, we provide sharp parameter selection criteria for the graded mesh, such that the optimal convergence rate is recovered for the associated FV solutions in the H^1-norm. The L^2 error estimate for a linear FV algorithm is summarized in Corollary 3.11. In Section 4, we report numerical results from both linear and quadratic FV schemes. These results are in strong agreement with our theoretical prediction, and hence verify the theory.

Throughout the paper, by $a \simeq b$, we mean that there are constants $C_1, C_2 > 0$, independent of the mesh level, such that $C_1 b \leq a \leq C_2 b$. The generic constant $C > 0$ in our analysis below may be different at different occurrences. It will depend on the computational domain, but not on the functions involved in the estimates or the mesh level in the FV algorithms.

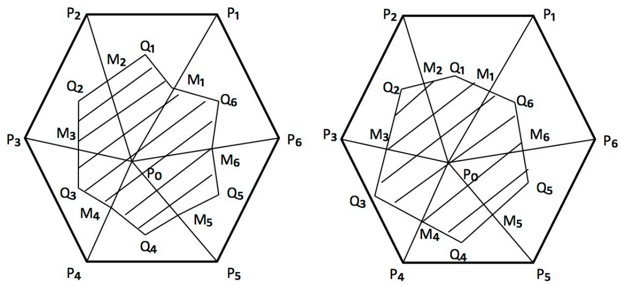

FIGURE 1. The barycenter control volume (left) and the circumcenter control volume (right). The control volume D_{P_0} is the polygon surrounded by the line segments $M_1Q_1M_2Q_2\ldots M_6Q_6M_1$, where M_i is the midpoint of the edge $P_0P_i, i = 1, \ldots, 6$.

2. Linear and quadratic FV schemes on graded meshes

In this section, we introduce the linear and quadratic FVMs associated with a family of graded mesh. We also summarize properties of the numerical algorithms that are useful for further analysis.

2.1. Linear and quadratic FVMs. Let $\mathcal{T}$ be a conforming, shape-regular, but not necessary quasi-uniform triangulation of Ω. With respect to $\mathcal{T}$, we recall the Lagrange finite element space

$$U_{\mathcal{T}} = \Big\{ v \in C(\overline{\Omega}) : v|_\tau \in \mathbf{P}_k, \quad \text{for all } \tau \in \mathcal{T}, \quad v|_{\partial\Omega} = 0 \Big\}, \tag{4}$$

where $k = 1, 2$ and $\mathbf{P}_k$ is the set of all polynomials of degree $\leq k$. It is clear that $U_{\mathcal{T}} \subset H_0^1(\Omega)$. Now suppose that $\mathcal{T}'$ is another partition (dual mesh) of Ω. Each element $\tau' \in \mathcal{T}'$ is often called a *control volume* and it is chosen to be a polygon. We require that if two control volumes intersect, they either share a vertex or an edge in $\mathcal{T}'$. Let $V_{\mathcal{T}'}$ be the piecewise constant function space with respect to $\mathcal{T}'$ defined by

$$V_{\mathcal{T}'} = \Big\{ v \in L^2(\overline{\Omega}) : v|_{\tau'} = \text{constant} \quad \text{for all } \tau' \in \mathcal{T}' \Big\}. \tag{5}$$

Normally, we require that $\dim(U_{\mathcal{T}}) = \dim(V_{\mathcal{T}'})$ and call $U_{\mathcal{T}}$ *the trial space* and $V_{\mathcal{T}'}$ *the test space*, respectively.

The construction of the dual mesh $\mathcal{T}'$ plays a critical role in the design of FV schemes. In this paper, we consider the following constructions of control volumes in $\mathcal{T}'$ for the linear ($k = 1$) and quadratic ($k = 2$) schemes.

Definition 2.1. (Control Volumes for $k = 1$). Let $\tau \in \mathcal{T}$ be a triangle. Associated with each vertex in $\mathcal{T}$, a common construction of the control volume is obtained by connecting some prechosen interior point $Q \in \tau$ to the midpoint of each edge of τ. In particular, we consider the following two constructions. When Q is chosen as the barycenter of the triangle, $\mathcal{T}'$ is the *barycenter dual mesh* [24], (see Figure 1 for a control volume); and when Q is chosen as the circumcenter of the triangle, $\mathcal{T}'$ becomes the *circumcenter dual mesh* [37] (see Figure 1).

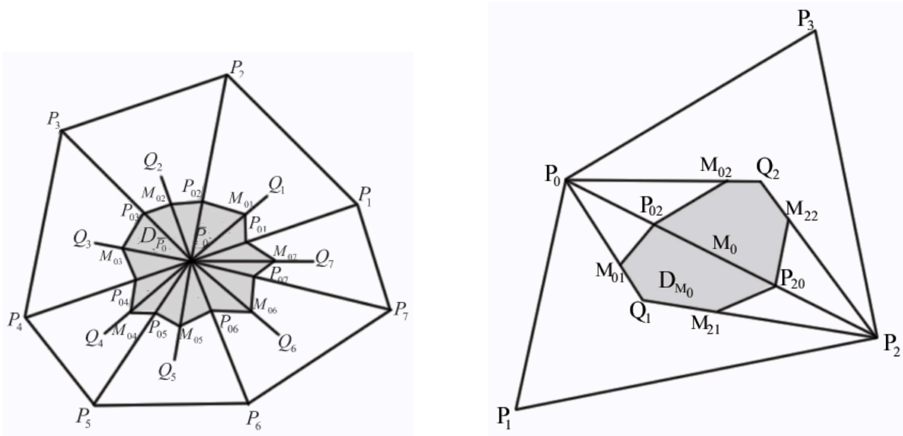

FIGURE 2. A control volume D_{P_0} (left) and a control volume D_{M_0} (right).

Definition 2.2. (Control Volumes for $k = 2$). For the quadratic dual mesh, we not only construct a *control volume* D_{P_0} for each interior vertex P_0 of $\mathcal{T}$, but also construct a *control volume* D_{M_0} for the midpoint M_0 of each internal edge E in $\mathcal{T}$. In Figure 2, we illustrate the construction of a class of control volumes for quadratic FV schemes on triangular meshes: (I) In the control volume D_{P_0},

$$\left|P_0P_{0i}\right| = \alpha\left|P_0P_i\right|, \quad \left|P_0M_{0i}\right| = \frac{3}{2}\beta\left|P_0Q_i\right|, \quad 1 \le i \le 7,$$

where $0 < \alpha < \frac{1}{2}, 0 < \beta < \frac{2}{3}$ are two given parameters and Q_i is the barycenter of the triangle. (II) In the control volume D_{M_0},

$$\left|P_0M_{0i}\right| = \frac{3}{2}\beta\left|P_0Q_i\right|,\ i = 1,2 \quad \text{and} \quad \left|P_2M_{1i}\right| = \frac{3}{2}\beta\left|P_2Q_i\right|,\ i = 1,2.$$

We shall in particular consider the following choices of α and β that lead to different FV schemes. The case $\alpha = \beta$ produces a very simple partition: $D_{P_0} \cap \tau$ is a triangle homothetic to τ, and $D_{M_0} \cap \tau$ is a pentagon. Li, Chen and Wu considered in [34] an FV scheme corresponding to $\alpha = \beta = 1/3$. For the case $\alpha \neq \beta$, we refer to Liebau [35] for $\alpha = 1/4, \beta = 1/3$ and Emonot [16] for $\alpha = 1/6, \beta = 1/4$.

It is clear that for a given triangulation $\mathcal{T}$, the trial space $U_{\mathcal{T}}$ always belongs to the *broken* Sobolev space $H^2_{\mathcal{T}}(\Omega)$ consisting of functions that are piecewise H^2 with respect to $\mathcal{T}$. We also note that in both cases ($k = 1, 2$), each control volume from the above constructions is associated with an interior *node* in the triangulation $\mathcal{T}$, namely, a vertex in the linear FVMs and a vertex or a midpoint on the edge in the quadratic FVMs.

From now on, we shall denote by $\mathcal{T}'$ one of the dual meshes defined in Definitions 2.1 and 2.2. For the trial space $U_{\mathcal{T}}$ in (4), we choose its degree $k = 1$ if $\mathcal{T}'$ is from Definition 2.1; and $k = 2$ if $\mathcal{T}'$ is from Definition 2.2. We shall also modify the test space in (5), such that

$$V_{\mathcal{T}'} = \Big\{ v \in L^2(\overline{\Omega}) : v|_{\tau'} = \text{constant for all } \tau' \in \mathcal{T}',\ v|_{\partial\Omega} = 0 \Big\}. \tag{6}$$

Thus, the FVM solving (1) is defined as follows. Find $u_{\mathcal{T}} \in U_{\mathcal{T}}$ such that

$$\int_{\partial\tau'} \nabla u_{\mathcal{T}} \cdot \mathbf{n} ds + \int_{\tau'} f dx = 0 \ , \qquad \forall\ \tau' \in \mathcal{T}_0', \tag{7}$$

where $\mathcal{T}_0' \subset \mathcal{T}'$ is the union of control volumes associated with the interior nodes in the triangulation $\mathcal{T}$, and $\mathbf{n}$ is the unit normal outward vector to τ'.

Let $\mathcal{E}_{\mathcal{T}'}$ be the union of all interior edges in $\mathcal{T}'$. For an edge $E \in \mathcal{E}_{\mathcal{T}'}$, let $\tau_1', \tau_2' \in \mathcal{T}'$ be the two control volumes having the common edge E. Then, we denote by $\mathbf{n}_E$ the unit normal direction pointing from τ_1' to τ_2' and define the jump of a function $v_{\mathcal{T}'} \in V_{\mathcal{T}'}$ over E: $[v_{\mathcal{T}'}] = v_{\mathcal{T}'}|_{\tau_1} - v_{\mathcal{T}'}|_{\tau_2}$. Define the norm for $v_{\mathcal{T}'} \in V_{\mathcal{T}'}$

$$|v_{\mathcal{T}'}|_{\mathcal{T}'} = \Big(\sum_{E \in \mathcal{E}_{\mathcal{T}'}} h_E^{-1} \int_E [v_{\mathcal{T}'}]^2 ds \Big)^{1/2}, \tag{8}$$

where h_E is the length of E. Then, for any $v_{\mathcal{T}'} \in V_{\mathcal{T}'}$, the FV solution $u_{\mathcal{T}}$ in (7) satisfies

$$a_{\mathcal{T}}(u_{\mathcal{T}}, v_{\mathcal{T}'}) = \int_\Omega f v_{\mathcal{T}'} dx = (f, v_{\mathcal{T}'}), \tag{9}$$

where the bilinear form $a_{\mathcal{T}}(\cdot,\cdot)$ is defined for all $u \in H_0^1(\Omega) \cap W_p^2(\Omega)$, $p > 1$, as

$$a_{\mathcal{T}}(u, v_{\mathcal{T}'}) := - \sum_{E \in \mathcal{E}_{\mathcal{T}'}} \int_E \nabla u \cdot \mathbf{n}_E \, [v_{\mathcal{T}'}] \, ds. \tag{10}$$

Remark 2.3. Different choices of the interior point Q in Definition 2.1 do not affect the stability of the linear FV scheme. See [45] for a detailed explanation. Moreover, it has been shown in [45] that the quadratic FV scheme is stable if the minimal angle $\theta_0 \geq 7.11°$ for $\alpha = 1/6, \beta = 1/4$; if $\theta_0 \geq 9.98°$ for $\alpha = 1/4, \beta = 1/3$; and if $\theta_0 \geq 20.95°$ for $\alpha = \beta = 1/3$.

We now recall the following stability result from [45].

Theorem 2.4. *Let $\mathcal{T}$ be a shape regular conforming triangulation of Ω. Consider the linear ($k = 1$) and quadratic ($k = 2$) FV schemes. Suppose the mesh size in $\mathcal{T}$ is sufficiently small. Let $v_{\mathcal{T}} \in U_{\mathcal{T}}$. Then, the following estimate holds for the linear FVMs (Definition 2.1).*

$$\big|v_{\mathcal{T}}\big|_{H^1(\Omega)} \leq C \sup_{V_{\mathcal{T}'} \ni v_{\mathcal{T}'} \neq 0} \frac{a_{\mathcal{T}}(v_{\mathcal{T}}, v_{\mathcal{T}'})}{\big|v_{\mathcal{T}'}\big|_{\mathcal{T}'}}, \tag{11}$$

where the constant C is independent of the mesh size. In addition, if the minimal angle θ_0 is not too small, (11) also holds for the quadratic FVMs (Definition 2.2).

Remark 2.5. Due to the availability of the stability results, we only consider the linear and quadratic FV schemes mentioned above. However, our approach can also be used to analyze other stable high order FV methods.

2.2. Graded meshes. We give the construction of a family of graded meshes for the triangulation $\mathcal{T}$ of the domain, and discuss its geometric properties.

Definition 2.6. (Graded Refinements). Let $v_i \in \partial\Omega$, $1 \leq i \leq l$, be the ith vertex of Ω and $\mathcal{V} := \{v_i\}$ be the vertex set. Let $\mathcal{T}$ be a triangulation of Ω whose vertices include $\mathcal{V}$, such that no triangle in $\mathcal{T}$ has more than one of its vertices in $\mathcal{V}$. Define

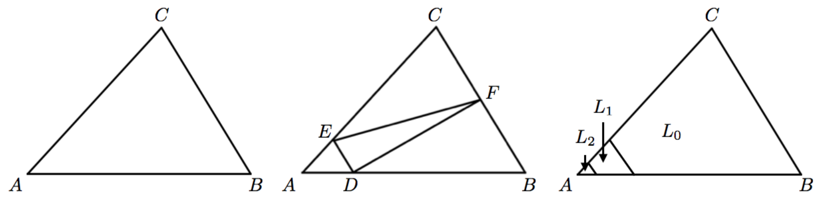

FIGURE 3. Graded triangulations and mesh layers (left – right): an initial triangle with $A \in \mathcal{V}$ and $B, C \notin \mathcal{V}$; one graded refinement to A, $\kappa_A = \frac{|AD|}{|AB|} = \frac{|AE|}{|AC|} = \frac{|DE|}{|BC|}$; three mesh layers resulted by two consecutive graded refinements toward A.

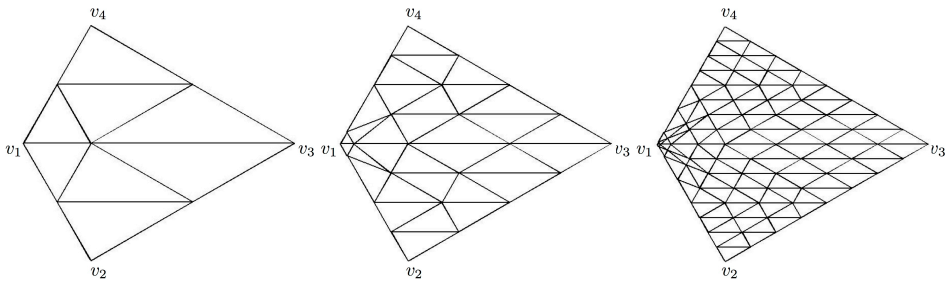

FIGURE 4. Three consecutive graded refinements of a polygonal domain with $\vec{\kappa} = (0.2, 0.5, 0.5, 0.5)$ (left – right): $\mathcal{T}_0$, the initial triangulation; $\mathcal{T}_1$, the mesh after one refinement; $\mathcal{T}_2$, the mesh after two refinements.

the vector $\vec{\kappa} = (\kappa_1, \kappa_2, \cdots, \kappa_l)$, for $\kappa_i \in (0, 1/2]$. Then, a $\vec{\kappa}$-refinement of $\mathcal{T}$, denoted by $\vec{\kappa}(\mathcal{T})$, is obtained by dividing each edge AB of $\mathcal{T}$ in two parts as follows:

- If neither A nor B is in $\mathcal{V}$, then we divide AB into two equal parts.
- Otherwise, if $A = v_i \in \mathcal{V}$, we divide AB into AC and CB such that $|AC| = \kappa_i|AB|$.

This will divide each triangle of $\mathcal{T}$ into four triangles (Figure 3). Given an initial triangulation $\mathcal{T}_0$, the associated family of graded triangulations $\{\mathcal{T}_j : j \geq 0\}$ is defined recursively, $\mathcal{T}_{j+1} = \vec{\kappa}(\mathcal{T}_j)$.

Remark 2.7. The grading parameter can be characterized in the following equation using the vector $\vec{c} = (c_1, c_2, \ldots, c_l)$

$$\kappa_i = 2^{-1/c_i}, \quad 1 \leq i \leq l, \ 0 < c_i \leq 1. \tag{12}$$

Therefore, $0 < \kappa_i \leq 1/2$ is completely determined by the vector $\vec{c}$. Note that in the case that $\kappa_i = 1/2$ ($c_i = 1$), we have a quasi-uniform triangulation near the vertex v_i; and when $\kappa_i < 1/2$ ($0 < c_i < 1$), we have the graded mesh near v_i.

A close examination of the graded mesh leads to our definition of mesh layers that are associated with these graded refinements toward the vertices.

Definition 2.8 (Mesh Layers)**.** Recall from Definition 2.6 that the triangulation $\mathcal{T}_j$, $0 \leq j \leq n$, is obtained after j successive graded refinements of $\mathcal{T}_0$ with parameter $\vec{\kappa}$. Let $\mathbb{T}_{i,j} \subset \mathcal{T}_j$, $1 \leq i \leq l$, be the union of (closed) triangles in $\mathcal{T}_j$ having $v_i \in \mathcal{V}$

as a vertex. Namely, $\mathbb{T}_{i,j}$ is the immediate neighborhood of v_i in $\mathcal{T}_j$. Define the regions near v_i, resulted from the graded refinement

$$L_{i,j} = \mathbb{T}_{i,j} \setminus \mathbb{T}_{i,j+1}, \text{ for } 0 \le j < n, \qquad \text{and} \qquad L_{i,n} = \mathbb{T}_{i,n},$$

Then, we denote the jth layer L_j, $0 \le j \le n$, of the mesh $\mathcal{T}_n$ by

$$L_j = \cup_{1 \le i \le l} L_{i,j}.$$

See Figure 3 for an illustration of mesh layers.

Remark 2.9. Let $\Omega_0 := \Omega \setminus \cup_i \mathbb{T}_{i,0}$. It is apparent that $\Omega = \Omega_0 \cup (\cup_{0 \le j \le n} L_j)$. Based on Definition 2.6, on the triangulation $\mathcal{T}_n$, the mesh size in $L_{i,j}$ is

$$h_{i,j} \simeq \kappa_i^j 2^{j-n}, \tag{13}$$

and the mesh size on Ω_0

$$h \simeq 2^{-n}. \tag{14}$$

In addition, the successive refinements in Definition 2.6 lead to the triangulation $\mathcal{T}_n$ with shape-regular triangles. The number of triangles in $\mathcal{T}_n$ is $O(4^n)$. Thus, the dimension of the associated linear and quadratic FVMs is $N \simeq 4^n$.

3. Error analysis

In this section, we give detailed regularity and error analysis for the proposed FVMs on graded meshes. This shall lead to a specific range for the grading parameter $\vec{\kappa}$, such that the associated FVMs approximate the singular solution in the optimal rate.

Throughout the rest of the paper, for simplicity, we denote the graded triangulation $\mathcal{T}_n$ by $\mathcal{T}$ and denote the dual mesh of $\mathcal{T}_n$ by $\mathcal{T}'$.

3.1. Weighted Sobolev spaces.

We first recall the following useful regularity results for (1) in Sobolev spaces (Section 2.7 in [21]).

Proposition 3.1. *Let ϕ_i be the interior angle of Ω at $v_i \in \mathcal{V}$ and define $\phi := \max_i(\phi_i)$. Then, the Laplace operator*

$$-\Delta : W_p^{m+2}(\Omega) \cap H_0^1(\Omega) \to W_p^m(\Omega), \quad m \ge 0,$$

defines an isomorphism, provided that the parameter p satisfies $1 < p < \eta_m$, where

$$\begin{cases} \eta_m = \infty & \text{for } \pi/\phi \ge m+2; \\ \eta_m = \frac{2}{m+2-\pi/\phi} & \text{for } \pi/\phi < m+2. \end{cases}$$

Therefore, the full regularity estimate (3) only holds for the values of m, such that $\eta_m > 2$. In particular, even for a smooth function f, the solution may not be in H^2 when the domain has re-entrant corners ($\phi > \pi$); and not in H^3 when $\phi > \pi/2$. These singular solutions, however, can be well described using the following spaces with special weights.

Let ℓ be the smallest distance from one vertex in $\mathcal{V}$ to a disjoint edge of Ω. Define the neighborhood of $v_i \in \mathcal{V}$, $\omega_i := B(v_i, \ell/4)$, where $B(v_i, \ell/4)$ is the ball centered at v_i with radius $\ell/4$. It is clear that $\omega_i \cap \omega_j = \emptyset$ for $i \ne j$.

Definition 3.2. (Weighted Sobolev Spaces). Let $r_i(x) \in C^\infty(\Omega)$ be a smooth function such that $r_i(x) =$ the distance from x to v_i if $x \in \omega_i$ and $r_i(x) = 1$ outside of $B(v_i, \ell/2)$. Let $\vec{\mu} := (\mu_1, \mu_2, \cdots, \mu_l)$ be an l-dimensional vector. For a constant c, we denote $c \pm \vec{\mu} := (c \pm \mu_1, c \pm \mu_2, \cdots, c \pm \mu_l)$. Then, we define the function

$$\rho(x) := \prod_{1 \le i \le l} r_i(x),$$

and its vector exponents

$$\rho^{c \pm \vec{\mu}}(x) := \prod_{1 \le i \le l} r_i(x)^{c \pm \mu_i} = \rho^c \prod_{1 \le i \le l} r_i(x)^{\pm \mu_i}.$$

Then, the weighted Sobolev space is

$$\mathcal{K}^m_{\vec{\mu}}(\Omega) := \{\rho^{|\alpha| - \vec{\mu}} \partial^\alpha v \in L^2(\Omega) \text{ for all } |\alpha| \le m\},$$

with norms and semi-norms

$$|v|_{\mathcal{K}^m_{\vec{\mu}}(\Omega)} := \left(\sum_{|\alpha| = m} \|\rho^{m - \vec{\mu}} \partial^\alpha v\|^2_{L^2(\Omega)} \right)^{1/2}, \quad \|v\|_{\mathcal{K}^m_{\vec{\mu}}(\Omega)} := \left(\sum_{|\alpha| \le m} |v|^2_{\mathcal{K}^m_{\vec{\mu}}(\Omega)} \right)^{1/2}.$$

Remark 3.3. Weighted spaces of this type are widely used [14, 13, 27, 26] to describe the local property of the singular solution near the vertex set $\mathcal{V}$. For example, in the region close to the vertex v_i, the weight in the space $\mathcal{K}^m_{\vec{\mu}}$ is determined only by the distance function $r_i(x)$ and the ith component μ_i of the vector $\vec{\mu}$. We also see that in a region that is away from the vertices, the $\mathcal{K}^m_{\vec{\mu}}$ is equivalent to H^m, because the weight is bounded above and below based on Definition 3.2. Recall the mesh layers in Definition 2.8. Then, the function ρ satisfies

$$\rho(x)|_{L_{i,j}} \simeq \kappa_i^j, \quad 0 \le j < n; \qquad \rho(x)|_{L_{i,n}} \le C\kappa_i^n. \tag{15}$$

In contrast to Proposition 3.1, we have the following full regularity estimates in these weighted spaces [33].

Proposition 3.4. *Let ϕ_i be the interior angle associated with the ith vertex v_i and $\vec{a} := (a_1, a_2, \cdots, a_l)$. Then, for $0 \le a_i < \pi/\phi_i$, if $f \in \mathcal{K}^m_{\vec{a}-1}(\Omega)$, the variational solution of equation (1) satisfies*

$$\|u\|_{\mathcal{K}^{m+2}_{\vec{a}+1}(\Omega)} \le C\|f\|_{\mathcal{K}^m_{\vec{a}-1}(\Omega)}. \tag{16}$$

We shall investigate the FV approximations in the weighted space.

3.2. Interpolation error estimates. We first introduce the dilation of a function in the neighborhood of a vertex in order to study the local behavior of the singular solution. Recall the neighborhood ω_i of the vertex v_i in Definition 3.2. Let $\sigma_i \subset \omega_i$ be a subset. We use a new coordinate system near v_i, which is a simple translation of the old xy-coordinate system, but with v_i as the new origin. Choose $0 < \lambda < 1$, such that on $\hat{\sigma}_i := \lambda^{-1}\sigma_i \subset \omega_i$. Therefore, ρ is still the distance to v_i on $\hat{\sigma}_i$. Then, we define the dilation of a function $v(x, y)$ as follows,

$$\hat{v}(\hat{x}, \hat{y}) := v(x, y), \qquad \forall\ (x, y) \in \sigma_i, \tag{17}$$

where $(\hat{x}, \hat{y}) := (\lambda^{-1}x, \lambda^{-1}y) \in \hat{\sigma}_i$.

Recall the notation $\mathcal{T} = \mathcal{T}_n$ for the graded mesh. In the subsequent estimates, we shall denote by h_E and h_τ the length of the edge $E \in \mathcal{E}_{\mathcal{T}'}$ and the size of the triangle $\tau \in \mathcal{T}$, respectively. Then, we have the following dilation estimates near the vertex in weighted spaces.

Lemma 3.5. *Let $E \in \mathcal{E}_{\mathcal{T}'}$ be an interior edge in the dual mesh near the vertex v_i, and let $\tau_E \in \mathcal{T}$ be the triangle, such that $E \subset \tau_E$, $\tau_E \subset \omega_i$. Choose $\lambda < 1$, such that $\hat{\tau}_E \in \omega_i$. Then, for $a \in \mathbb{R}^+$ and $m \in \mathbb{Z}_{\geq 0}$, we have*

$$\|\rho^{m-a}\nabla^m_{(x,y)} v\|_{L^2(\tau_E)} = \lambda^{1-a}\|\rho^{m-a}\nabla^m_{(\hat{x},\hat{y})}\hat{v}\|_{L^2(\hat{\tau}_E)}, \tag{18}$$

$$\|\rho^{1/2-a}\nabla_{(x,y)} v\|_{L^2(E)} = \lambda^{-a}\|\rho^{1/2-a}\nabla_{(\hat{x},\hat{y})}\hat{v}\|_{L^2(\hat{E})}, \tag{19}$$

$$\|\rho^{-1/2+a}\left[v_{\mathcal{T}'}\right]\|_{L^2(E)} \leq C\lambda^{a-1/2}h_E^{1/2}|v_{\mathcal{T}'}|_{\mathcal{T}'(E)}, \quad \forall\ v_{\mathcal{T}'} \in V_{\mathcal{T}'}, \tag{20}$$

where $\nabla^m_{(x,y)}$ denotes the vector of all mth-order derivatives in terms of x and y; and $|v_{\mathcal{T}'}|^2_{\mathcal{T}'(E)} := h_E^{-1}\int_E \left[v_{\mathcal{T}'}\right]^2 ds$.

Proof. Recall that ρ is the distance to v_i in τ_E and $\hat{\tau}_E$. Therefore, $\rho(x,y) = \lambda\rho(\hat{x},\hat{y})$. Then, by (17) and the scaling argument, we first show (18) as follows.

$$\begin{aligned}
\|\rho^{m-a}\nabla^m_{(\hat{x},\hat{y})}\hat{v}\|^2_{L^2(\hat{\tau}_E)} &= \sum_{j+k=m}\int_{\hat{\tau}_E}|\rho^{m-a}(\hat{x},\hat{y})\partial^j_{\hat{x}}\partial^k_{\hat{y}}\hat{v}(\hat{x},\hat{y})|^2 d\hat{x}d\hat{y}\\
&= \sum_{j+k=m}\int_{\tau_E}|\lambda^{a-m}\rho^{m-a}(x,y)\lambda^m\partial^j_x\partial^k_y v(x,y)|^2\lambda^{-2}dxdy\\
&= \lambda^{2a-2}\sum_{j+k=m}\int_{\tau_E}|\rho^{m-a}(x,y)\partial^j_x\partial^k_y v(x,y)|^2 dxdy\\
&= \lambda^{2a-2}\|\rho^{m-a}\nabla^m_{(x,y)}v\|^2_{L^2(\tau_E)}.
\end{aligned}$$

We prove (19) with a similar calculation,

$$\begin{aligned}
\|\rho^{1/2-a}\nabla_{(x,y)}v\|^2_{L^2(E)} &= \sum_{j+k=1}\int_E|\rho^{1/2-a}(x,y)\partial^j_x\partial^k_y v(x,y)|^2 ds\\
&= \sum_{j+k=1}\int_{\hat{E}}|\lambda^{1/2-a}\rho^{1/2-a}(\hat{x},\hat{y})\lambda^{-1}\partial^j_{\hat{x}}\partial^k_{\hat{y}}v(\hat{x},\hat{y})|^2\lambda d\hat{s}\\
&= \lambda^{-2a}\|\rho^{1/2-a}\nabla_{(\hat{x},\hat{y})}\hat{v}\|^2_{L^2(\hat{E})}.
\end{aligned}$$

For (20), recall that $[v_{\mathcal{T}'}]$ is constant on E. Then, by the scaling argument, we first have

$$\|\rho^{-1/2+a}\left[v_{\mathcal{T}'}\right]\|^2_{L^2(E)} = \lambda^{2a}\int_{\hat{E}}|\rho^{-1/2+a}(\hat{x},\hat{y})\left[v_{\mathcal{T}'}\right]|^2 d\hat{s}.$$

Note that both $(\int_{\hat{E}}|\rho^{-1/2+a}\left[v_{\mathcal{T}'}\right]|^2 d\hat{s})^{1/2}$ and $(\int_{\hat{E}}|\left[v_{\mathcal{T}'}\right]|^2 d\hat{s})^{1/2}$ are norms of $[v_{\mathcal{T}'}]$. By the norm equivalence on finite dimensional spaces and the scaling argument, we have

$$\begin{aligned}
\|\rho^{-1/2+a}\left[v_{\mathcal{T}'}\right]\|^2_{L^2(E)} &\leq C\lambda^{2a}\int_{\hat{E}}|\left[v_{\mathcal{T}'}\right]|^2 d\hat{s}\\
&= C\lambda^{2a-1}\int_E|\left[v_{\mathcal{T}'}\right]|^2 ds = C\lambda^{2a-1}h_E|v_{\mathcal{T}'}|^2_{\mathcal{T}'(E)}.
\end{aligned}$$

This completes the proof for (20). $\square$

Recall the mesh layers in Definition 2.8 and that $k = 1, 2$, is the degree of polynomials on each $\tau \in \mathcal{T}$ for the trial space (4). Recall that ϕ_i is the interior angle of Ω at v_i and recall the grading parameter $\kappa_i = 2^{-1/c_i}$, $0 < c_i \leq 1$. For $w \in \mathcal{K}^{k+1}_{\vec{a}+1}(\Omega)$, let $w_I \in U_{\mathcal{T}}$ be its nodal interpolation, where $\vec{a} = (a_1, a_2, \ldots, a_l)$, $a_i \geq 0$. This makes sense since by the Sobolev embedding Theorem, w is continuous on any interior sub-region that is away from the vertices. Then, we have the local interpolation error estimate in the weighted space.

Theorem 3.6. *Suppose $w \in \mathcal{K}^{k+1}_{\vec{a}+1}(\Omega)$, for $0 < a_i < \frac{\pi}{\phi_i}$. Choose the grading parameter $\vec{\kappa}$ in (12), such that $0 < c_i \leq a_i$ for $k = 1$, and $0 < c_i \leq a_i/2$ for $k = 2$. Let $N := \dim(U_{\mathcal{T}}) \simeq 4^n$. Then, for any $\tau \in \mathcal{T}$, we have*

$$\|w - w_I\|_{H^1(\tau)} \leq CN^{-k/2}\|w\|_{\mathcal{K}^{k+1}_{\vec{a}+1}(\tau)}. \tag{21}$$

In addition, for $\tau \subset L_{i,n}$,

$$h_\tau^{c_i}\|\rho^{-c_i}\nabla(w - w_I)\|_{L^2(\tau)} \leq CN^{-k/2}\|w\|_{\mathcal{K}^{k+1}_{\vec{a}+1}(\tau)}, \tag{22}$$

$$h_\tau^{c_i}\|\rho^{1-c_i}\nabla^2(w - w_I)\|_{L^2(\tau)} \leq CN^{-k/2}\|w\|_{\mathcal{K}^{k+1}_{\vec{a}+1}(\tau)}. \tag{23}$$

Proof. We first consider the case $\tau \not\subset L_n$. Note that for $\tau \subset \Omega_0$, (21) is an immediate consequence of the usual interpolation error estimate in usual Sobolev spaces, (14), and the fact $\rho = \mathcal{O}(1)$. For $\tau \subset L_{i,j}$, $j < n$, by (15), we have $w \in H^{k+1}(\tau)$ and $\rho \simeq \kappa_i^j$. Therefore, by the usual interpolation error estimate, (13), and (12), we have

$$\begin{aligned} \|w - w_I\|_{H^1(\tau)} &\leq Ch_\tau^k|w|_{H^{k+1}(\tau)} \leq C2^{-nk}\|\kappa_i^{jk}2^{jk}\nabla^{k+1}w\|_{L^2(\tau)} \\ &\leq CN^{-k/2}\|\rho^{k-a_i}\nabla^{k+1}w\|_{L^2(\tau)} \leq CN^{-k/2}\|w\|_{\mathcal{K}^{k+1}_{\vec{a}+1}(\tau)}. \end{aligned} \tag{24}$$

For estimates on $\tau \subset L_{i,n}$, we introduce χ, a smooth cutoff function on τ such that $\chi = 0$ in a neighborhood of v_i and $= 1$ at every other node of τ. Therefore,

$$w_I = (\chi w)_I. \tag{25}$$

Apply the dilation in (17) to τ. Choose $\lambda \simeq h_\tau$, such that ρ is still the distance to v_i on $\hat{\tau}$. Define $\hat{v} := \hat{w} - \hat{\chi}\hat{w}$. Then, for $\beta = 0$ or c_i, we have,

$$\begin{aligned} \|\rho^{-\beta}\nabla(\hat{w} - \hat{w}_I)\|_{L^2(\hat{\tau})} &= \|\rho^{-\beta}\nabla(\hat{v} + \hat{\chi}\hat{w} - \hat{w}_I)\|_{L^2(\hat{\tau})} \\ &\leq \|\rho^{-\beta}\nabla\hat{v}\|_{L^2(\hat{\tau})} + \|\rho^{-\beta}\nabla(\hat{\chi}\hat{w} - \hat{w}_I)\|_{L^2(\hat{\tau})}. \end{aligned} \tag{26}$$

Similarly, we have

$$\|\rho^{1-c_i}\nabla^2(\hat{w} - \hat{w}_I)\|_{L^2(\hat{\tau})} \leq \|\rho^{1-c_i}\nabla^2\hat{v}\|_{L^2(\hat{\tau})} + \|\rho^{1-c_i}\nabla^2(\hat{\chi}\hat{w} - \hat{w}_I)\|_{L^2(\hat{\tau})}. \tag{27}$$

Let $\vec{b}$ be an l-dimensional vector, such at $b_j = a_j$ for $1 \leq j \leq l$, $j \neq i$. We shall choose different values for b_i in the subsequent estimates. For $b_i = \beta$, since $\hat{\chi} \in C^\infty(\hat{\tau})$ and vanishes near v_i, we have

$$\|\rho^{-\beta}\nabla\hat{v}\|_{L^2(\hat{\tau})} \leq \|\hat{v}\|_{\mathcal{K}^{k+1}_{\vec{b}+1}(\hat{\tau})} \leq \|\hat{w}\|_{\mathcal{K}^{k+1}_{\vec{b}+1}(\hat{\tau})} + \|\hat{\chi}\hat{w}\|_{\mathcal{K}^{k+1}_{\vec{b}+1}(\hat{\tau})} \leq C\|\hat{w}\|_{\mathcal{K}^{k+1}_{\vec{b}+1}(\hat{\tau})}, \tag{28}$$

where C depends on the shape of $\hat{\tau}$ through $\hat{\chi}$. Following the same procedure, for $b_i = c_i$, we also have

$$\|\rho^{1-c_i}\nabla^2\hat{v}\|_{L^2(\hat{\tau})} \leq C\|\hat{w}\|_{\mathcal{K}^{k+1}_{\vec{b}+1}(\hat{\tau})}. \tag{29}$$

Then, using (18), (26), (28), (25), and the usual interpolation error estimate, for $\tau \in L_{i,n}$ and $b_i = \beta$, we have

$$
\begin{aligned}
\|\rho^{-\beta}\nabla(w - w_I)\|_{L^2(\tau)} &\le Ch_\tau^{-\beta}\|\rho^{-\beta}\nabla(\hat{w} - \hat{w}_I)\|_{L^2(\hat{\tau})} \\
&\le Ch_\tau^{-\beta}(\|\hat{w}\|_{\mathcal{K}^{k+1}_{\vec{b}+1}(\hat{\tau})} + \|\rho^{-\beta}\nabla(\hat{\chi}\hat{w} - (\hat{\chi}\hat{w})_I)\|_{L^2(\hat{\tau})}) \\
&\le Ch_\tau^{-\beta}(\|\hat{w}\|_{\mathcal{K}^{k+1}_{\vec{b}+1}(\hat{\tau})} + \|\nabla(\hat{\chi}\hat{w} - (\hat{\chi}\hat{w})_I)\|_{L^2(\hat{\tau})}) \\
&\le Ch_\tau^{-\beta}(\|\hat{w}\|_{\mathcal{K}^{k+1}_{\vec{b}+1}(\hat{\tau})} + \|\hat{\chi}\hat{w}\|_{H^{k+1}(\hat{\tau})}) \\
&\le Ch_\tau^{-\beta}\|\hat{w}\|_{\mathcal{K}^{k+1}_{\vec{b}+1}(\hat{\tau})} \le C\|w\|_{\mathcal{K}^{k+1}_{\vec{b}+1}(\tau)}. \qquad (30)
\end{aligned}
$$

Using (18), (27), (29), for $b_i = c_i$, a similar calculation leads to the following estimates.

$$
\begin{aligned}
\|\rho^{1-c_i}\nabla^2(w - w_I)\|_{L^2(\tau)} &\le Ch_\tau^{-c_i}\|\rho^{1-c_i}\nabla^2(\hat{w} - \hat{w}_I)\|_{L^2(\hat{\tau})} \\
&\le Ch_\tau^{-c_i}(\|\hat{w}\|_{\mathcal{K}^{k+1}_{\vec{b}+1}(\hat{\tau})} + \|\rho^{1-c_i}\nabla^2(\hat{\chi}\hat{w} - (\hat{\chi}\hat{w})_I)\|_{L^2(\hat{\tau})}) \\
&\le Ch_\tau^{-c_i}(\|\hat{w}\|_{\mathcal{K}^{k+1}_{\vec{b}+1}(\hat{\tau})} + \|\nabla^2(\hat{\chi}\hat{w} - (\hat{\chi}\hat{w})_I)\|_{L^2(\hat{\tau})}) \\
&\le Ch_\tau^{-c_i}(\|\hat{w}\|_{\mathcal{K}^{k+1}_{\vec{b}+1}(\hat{\tau})} + \|\hat{\chi}\hat{w}\|_{H^{k+1}(\hat{\tau})}) \\
&\le Ch_\tau^{-c_i}\|\hat{w}\|_{\mathcal{K}^{k+1}_{\vec{b}+1}(\hat{\tau})} \le C\|w\|_{\mathcal{K}^{k+1}_{\vec{b}+1}(\tau)}. \qquad (31)
\end{aligned}
$$

Recall from (13) $h_\tau \simeq \kappa_i^n = 2^{-n/c_i}$. Therefore, in the case $b_i = \beta = 0$, for $\tau \subset L_{i,n}$, by (30), we have

$$
\|\nabla(w - w_I)\|_{L^2(\tau)} \le C\|w\|_{\mathcal{K}^{k+1}_{\vec{b}+1}(\tau)} \le Ch_\tau^{a_i}\|w\|_{\mathcal{K}^{k+1}_{\vec{a}+1}(\tau)} \le CN^{-k/2}\|w\|_{\mathcal{K}^{k+1}_{\vec{a}+1}(\tau)}.
$$

This together with (24) proves (21).

In the case $b_i = \beta = c_i$, for $\tau \subset L_{i,n}$, by (30), we have

$$
\begin{aligned}
h_\tau^{c_i}\|\rho^{-c_i}\nabla(w - w_I)\|_{L^2(\tau)} &\le Ch_\tau^{c_i}\|w\|_{\mathcal{K}^{k+1}_{\vec{b}+1}(\tau)} \\
&\le Ch_\tau^{kc_i}\|w\|_{\mathcal{K}^{k+1}_{\vec{a}+1}(\tau)} \le CN^{-k/2}\|w\|_{\mathcal{K}^{k+1}_{\vec{a}+1}(\tau)}.
\end{aligned}
$$

This proves (22).

By (31) and $b_i = c_i$, we have

$$
\begin{aligned}
h_\tau^{c_i}\|\rho^{1-c_i}\nabla^2(w - w_I)\|_{L^2(\tau)} &\le Ch_\tau^{c_i}\|w\|_{\mathcal{K}^{k+1}_{\vec{b}+1}(\tau)} \\
&\le Ch_\tau^{kc_i}\|w\|_{\mathcal{K}^{k+1}_{\vec{a}+1}(\tau)} \le CN^{-k/2}\|w\|_{\mathcal{K}^{k+1}_{\vec{a}+1}(\tau)}.
\end{aligned}
$$

This proves (23). □

3.3. Continuity of the FV bilinear form in weighted spaces. Recall that for any $w \in \mathcal{K}^2_{\vec{a}+1}(\Omega)$, $w \in H^2(G)$ for any region G that is away from the vertex set $\mathcal{V}$. Then, we study the continuity of the bilinear form $a_{\mathcal{T}}(\cdot,\cdot)$ in (10) in order to analyze the convergence of the FVM on graded meshes.

Lemma 3.7. *For an edge $E \in \mathcal{E}_{\mathcal{T}'}$, let $\tau_E \in \mathcal{T}$ be the triangle, such that $E \subset \tau_E$. Then, for any $w \in H^2(\tau_E)$, we have*

$$
\sup \int_E \nabla w \cdot \mathbf{n}_E\,[v_{\mathcal{T}'}]\,ds \le C(\|\nabla w\|_{L^2(\tau_E)} + h_E|\nabla^2 w|_{L^2(\tau_E)})|v_{\mathcal{T}'}|_{\mathcal{T}'(E)}, \qquad (32)
$$

where $|v_{\mathcal{T}'}|_{\mathcal{T}'(E)} := h_E^{-1/2}(\int_E [v_{\mathcal{T}'}]^2 ds)^{1/2}$*; and if* $\tau_E \cap v_i \neq \emptyset$ *and* $w \in \mathcal{K}^2_{\vec{a}+1}(\tau_E)$*,* $a_i > 0$*, then we have*

$$\sup \int_E \nabla w \cdot \mathbf{n}_E \,[v_{\mathcal{T}'}]\, ds \leq C h_E^{a_i} (\|\rho^{-a_i}\nabla w\|_{L^2(\tau_E)} + \|\rho^{1-a_i}\nabla^2 w\|_{L^2(\tau_E)}) |v_{\mathcal{T}'}|_{\mathcal{T}'(E)}. \tag{33}$$

Proof. (32) can be proved by Hölder's inequality and the trace estimate,

$$\begin{aligned}
\int_E |\nabla w \cdot \mathbf{n}_E \,[v_{\mathcal{T}'}]\, | ds &\leq \|\nabla w\|_{L^2(E)} \| \,[v_{\mathcal{T}'}]\, \|_{L^2(E)} \\
&\leq C(h_E^{-1/2}\|\nabla w\|_{L^2(\tau_E)} + h_E^{1/2}\|\nabla^2 w\|_{L^2(\tau_E)}) h_E^{1/2} |v_{\mathcal{T}'}|_{\mathcal{T}'(E)} \\
&\leq C(\|\nabla w\|_{L^2(\tau_E)} + h_E|\nabla^2 w|_{L^2(\tau_E)}) |v_{\mathcal{T}'}|_{\mathcal{T}'(E)}.
\end{aligned}$$

If $\tau_E \cap v_i \neq \emptyset$, recall any edge $E \in \mathcal{E}_{\mathcal{T}'}$ does not touch the vertex set $\mathcal{V}$. Let $\tau'_E \in \mathcal{T}'$ be the control volume such that $E \subset \partial\tau'_E$ and τ'_E is associated with an interior node of the triangulation $\mathcal{T}$. Denote by $\mathfrak{I} := \tau_E \cap \tau'_E$ the intersection. Therefore, $\rho(x) \simeq h_E$ for any $x \in \mathfrak{I}$. We choose $\lambda \simeq h_E$ in (17), such that $\hat{\tau}_E \subset \omega_i$ has diameter $\mathcal{O}(1)$. Then, by Hölder's inequality, (19), (20), the trace estimate, and (18), we have

$$\begin{aligned}
\int_E |\nabla w \cdot \mathbf{n}_E \,[v_{\mathcal{T}'}]\, | ds &\leq \|\rho^{1/2}\nabla w\|_{L^2(E)} \|\rho^{-1/2} \,[v_{\mathcal{T}'}]\, \|_{L^2(E)} \\
&\leq C\|\nabla_{(\hat{x},\hat{y})}\hat{w}\|_{L^2(\hat{E})} |v_{\mathcal{T}'}|_{\mathcal{T}'(E)} \\
&\leq C(\|\nabla_{(\hat{x},\hat{y})}\hat{w}\|_{L^2(\hat{\mathfrak{I}})} + \|\nabla^2_{(\hat{x},\hat{y})}\hat{w}\|_{L^2(\hat{\mathfrak{I}})}) |v_{\mathcal{T}'}|_{\mathcal{T}'(E)} \\
&\leq C h_E^{a_i} (\|\rho^{-a_i}\nabla w\|_{L^2(\mathfrak{I})} + \|\rho^{1-a_i}\nabla^2 w\|_{L^2(\mathfrak{I})}) |v_{\mathcal{T}'}|_{\mathcal{T}'(E)} \\
&\leq C h_E^{a_i} (\|\rho^{-a_i}\nabla w\|_{L^2(\tau_E)} + \|\rho^{1-a_i}\nabla^2 w\|_{L^2(\tau_E)}) |v_{\mathcal{T}'}|_{\mathcal{T}'(E)}.
\end{aligned}$$

This completes the proof for (33). □

Then, we have the following upper bound for the bilinear form $a_{\mathcal{T}}(\cdot,\cdot)$.

Lemma 3.8. *For the graded mesh* $\mathcal{T} := \mathcal{T}_n$*, recall the grading parameter* $\kappa_i = 2^{-1/c_i}$ *for* $0 < c_i \leq 1$ *in (12) and the mesh layer in Definition 2.8. Let* $\vec{c} := (c_1, c_2, \cdots, c_l)$*. Define*

$$R^2(w) := \sum_{\tau\in\mathcal{T}, \tau\not\subset L_n} (\|\nabla w\|^2_{L^2(\tau)} + N^{-1}\|\rho^{1-\vec{c}}\nabla^2 w\|^2_{L^2(\tau)})$$

and

$$S^2(w) := \sum_{1\leq i\leq l} \sum_{(\tau\in\mathcal{T}, \tau\subset L_{i,n})} h_\tau^{2c_i} (\|\rho^{-c_i}\nabla w\|^2_{L^2(\tau)} + \|\rho^{1-c_i}\nabla^2 w\|^2_{L^2(\tau)}).$$

Then, for $w \in \mathcal{K}^2_{\vec{c}+1}(\Omega)$*, we have*

$$a_{\mathcal{T}}(w, v_{\mathcal{T}'}) \leq C|v_{\mathcal{T}'}|_{\mathcal{T}'} \big(S^2(w) + R^2(w)\big)^{1/2}, \tag{34}$$

where $|v_{\mathcal{T}'}|_{\mathcal{T}'}$ *is the norm defined in (8).*

Proof. For $w \in \mathcal{K}^2_{\vec{c}+1}(\Omega)$, based on the definition of the weighted space, $w \in H^2(\tau)$ for $\tau \in \mathcal{T}$ and $\tau \not\subset L_n$. Then, by the Cauchy-Schwarz inequality and Lemma 3.7, we first have

$$a_{\mathcal{T}}(w, v_{\mathcal{T}'}) \le C|v_{\mathcal{T}'}|_{\mathcal{T}'}\big(S^2(w) + \sum_{\tau \not\subset L_n} (\|\nabla w\|^2_{L^2(\tau)} + h_\tau^2 \|\nabla^2 w\|^2_{L^2(\tau)})\big)^{1/2}.$$

Therefore, to prove (34), it is sufficient to show for any $\tau \not\subset L_n$

$$h_\tau^2 \|\nabla^2 w\|^2_{L^2(\tau)} \le CN^{-1}\|\rho^{1-\vec{c}}\nabla^2 w\|^2_{L^2(\tau)}. \tag{35}$$

Suppose $\tau \subset L_{i,j}$, $0 \le j < n$. Then by (13) and (15), $h_\tau^2 \simeq \kappa_i^{2j} 2^{2j-2n}$ and $\rho \simeq \kappa_i^j$ on τ. Thus, by (12), we have

$$h_\tau^2 \|\nabla^2 w\|^2_{L^2(\tau)} \le C2^{-2n}\|\kappa_i^j 2^j \nabla^2 w\|^2_{L^2(\tau)} \le CN^{-1}\|\rho^{1-c_i}\nabla^2 w\|^2_{L^2(\tau)}.$$

If $\tau \subset \Omega_0 := \Omega \setminus \cup_i \mathbb{T}_{i,0}$, we have $h_\tau \simeq 2^{-n} \simeq N^{-1/2}$ and $\rho(x) = \mathcal{O}(1)$ for $x \in \tau$. Then, (35) is proved by a straightforward calculation. $\square$

3.4. Convergence estimates for FVMs. We are now ready to provide the error analysis for the linear and quadratic FVMs on graded meshes. We first present our error estimate in the H^1-norm.

Theorem 3.9. *Suppose $f \in \mathcal{K}^{k-1}_{\vec{a}-1}(\Omega)$ in equation (1), $k = 1, 2$, where $0 < a_i < \pi/\phi_i$. Choose the grading parameter $\kappa_i = 2^{-1/c_i}$, $0 < c_i \le 1$, such that $0 < c_i \le a_i$ for $k = 1$ and $0 < c_i \le a_i/2$ for $k = 2$. Then, the FV solution $u_{\mathcal{T}} \in U_{\mathcal{T}}$ (9) satisfies*

$$\|u - u_{\mathcal{T}}\|_{H^1(\Omega)} \le CN^{-k/2}\|f\|_{\mathcal{K}^{k-1}_{\vec{a}-1}(\Omega)}, \tag{36}$$

where $N \simeq 4^n$ is the dimension of the trial space.

Proof. Given $f \in \mathcal{K}^{k-1}_{\vec{a}-1}(\Omega)$, by the regularity estimate (16), $u \in \mathcal{K}^{k+1}_{\vec{a}+1}(\Omega)$. Let $u_I \in U_{\mathcal{T}}$ be the nodal interpolation of u. Then,

$$\|u - u_{\mathcal{T}}\|_{H^1(\Omega)} \le \|u - u_I\|_{H^1(\Omega)} + \|u_{\mathcal{T}} - u_I\|_{H^1(\Omega)}. \tag{37}$$

By (11), (9), (10), and Lemma 3.8,

$$\begin{aligned} \|u_{\mathcal{T}} - u_I\|_{H^1(\Omega)} &\le C \sup_{V_{\mathcal{T}'} \ni v_{\mathcal{T}'} \ne 0} \frac{a_{\mathcal{T}}(u_{\mathcal{T}} - u_I, v_{\mathcal{T}'})}{|v_{\mathcal{T}'}|_{\mathcal{T}'}} \\ &= C \sup_{V_{\mathcal{T}'} \ni v_{\mathcal{T}'} \ne 0} \frac{a_{\mathcal{T}}(u - u_I, v_{\mathcal{T}'})}{|v_{\mathcal{T}'}|_{\mathcal{T}'}} \\ &\le C\big(R^2(u - u_I) + S^2(u - u_I)\big)^{1/2}. \end{aligned} \tag{38}$$

Note that for $k = 1$ and $\tau \not\subset L_n$,

$$N^{-1}\|\rho^{1-\vec{c}}\nabla^2(u - u_I)\|^2_{L^2(\tau)} \le CN^{-1}\|u\|_{\mathcal{K}^2_{\vec{c}+1}(\tau)} \le CN^{-1}\|u\|_{\mathcal{K}^2_{\vec{a}+1}(\tau)}.$$

This, together with (37), (38), Lemma 3.8, Theorem 3.6, and Proposition 3.4 completes the proof of (36) for the case $k = 1$.

For $k = 2$ and $\tau \not\subset L_n$, suppose $\tau \subset L_{i,j}$, $0 \le j < n$. Therefore, $\rho|_\tau \simeq \kappa_i^j$. By the usual interpolation error estimate, (12), (13), and the definition of the weighted space, we have

$$
\begin{aligned}
N^{-1}\|\rho^{1-\vec{c}}\nabla^2(u-u_I)\|^2_{L^2(\tau)} &\leq CN^{-1}\kappa_i^{2j(1-c_i)}\|\nabla^2(u-u_I)\|^2_{L^2(\tau)}\\
&\leq CN^{-1}h_\tau^2\kappa_i^{2j(1-c_i)}|u|^2_{H^3(\tau)} \leq CN^{-1}h_\tau^2\kappa_i^{j(2c_i-2)}\|\rho^{2-2c_i}\nabla^3 u\|^2_{L^2(\tau)}\\
&\leq CN^{-1}\kappa_i^{2j}2^{2j-2n}\kappa_i^{j(2c_i-2)}\|u\|^2_{\mathcal{K}^3_{2\vec{c}+1}(\tau)} \leq CN^{-2}\|u\|^2_{\mathcal{K}^3_{\vec{a}+1}(\tau)}.
\end{aligned}
$$

If $\tau \subset \Omega_0$, a straightforward calculation shows

$$
N^{-1}\|\rho^{1-\vec{c}}\nabla^2(u-u_I)\|^2_{L^2(\tau)} \leq CN^{-2}\|u\|^2_{\mathcal{K}^3_{\vec{a}+1}(\tau)}.
$$

This, together with (37), (38), Lemma 3.8, Theorem 3.6, and Proposition 3.4 completes the proof of (36) for the case $k = 2$. $\square$

Remark 3.10. In Theorem 3.9, we provide the selection criteria for the grading parameter $\vec{\kappa}$, such that the associated (linear and quadratic) FVMs approximate the singular solutions in the H^1-norm with the optimal convergence rate. The ingredients for the analysis include the stability of the FV bilinear form (Theorem 2.4), the continuity estimates (Lemma 3.8), and the interpolation error estimates (Theorem 3.6). These results extend to more general equations in the divergence form

$$
-\nabla\cdot(A\nabla u) = f \quad \text{in} \quad \Omega,
$$

provided that the function A is sufficiently smooth and appropriate boundary conditions are presented. Note that for boundary conditions different from the Dirichlet condition, new weighted spaces need to be introduced for the well-posedness and regularity of the singular solution [33]. This, however, will not affect our local interpolation estimates. Therefore, we expect similar results for these problems. In addition, given the stability of the scheme, these analytical tools can apply to other high order FVMs.

We further have the optimal L^2 error estimate for a linear FVM.

Corollary 3.11. *Suppose $f \in \mathcal{K}^1_{\vec{a}-1}(\Omega)$, $0 < a_i \leq 1$ and $0 < a_i < \pi/\phi_i$. Choose the parameter $\vec{c}$ as in Theorem 3.9 for $k = 1$. In the linear FVM, suppose the barycenter of each triangle and the midpoint of each edge are chosen to construct the control volume. Then, we have the following L^2 estimate on the graded mesh*

$$
\|u-u_{\mathcal{T}}\|_{L^2(\Omega)} \leq CN^{-1}\|f\|_{\mathcal{K}^1_{\vec{a}-1}(\Omega)}.
$$

Proof. Consider the following auxiliary equation

$$
-\Delta\psi = u - u_{\mathcal{T}} \quad \text{in} \quad \Omega, \qquad \psi = 0 \quad \text{on} \quad \partial\Omega. \tag{39}
$$

Let $\psi_I \in U_{\mathcal{T}}$ be the usual nodal interpolation of ψ. Let $\psi_{I'} \in V_{\mathcal{T}'}$ be such that $\psi_{I'}(p) = \psi_I(p)$ for any node p of the triangulation. Then, a direct calculation shows [10]

$$
\int_\tau(\psi_I - \psi_{I'})dx = 0, \qquad \forall\ \tau \in \mathcal{T}, \tag{40}
$$

$$
\int_e(\psi_I - \psi_{I'})ds = 0, \qquad \text{for any edge } e \text{ of } \tau \in \mathcal{T}. \tag{41}
$$

Note

$$\begin{aligned} \|u-u_{\mathcal{T}}\|^2_{L^2(\Omega)} &= \int_\Omega \nabla\psi\cdot\nabla(u-u_{\mathcal{T}})dx \\ &= \int_\Omega \nabla(\psi-\psi_I)\cdot\nabla(u-u_{\mathcal{T}})dx + \int_\Omega \nabla\psi_I\cdot\nabla(u-u_{\mathcal{T}})dx. \end{aligned} \tag{42}$$

By (2) and (9), we have

$$\int_\Omega \nabla\psi_I\cdot\nabla(u-u_{\mathcal{T}})dx = \int_\Omega f(\psi_I-\psi_{I'})dx + \int_\Omega f\psi_{I'}dx - \int_\Omega \nabla u_{\mathcal{T}}\cdot\nabla\psi_I dx$$

$$= \int_\Omega f(\psi_I-\psi_{I'})dx - \sum_{E\in\mathcal{E}_{\mathcal{T}'}}\int_E \nabla u_{\mathcal{T}}\cdot\mathbf{n}_E[\psi_{I'}]ds - \int_\Omega \nabla u_{\mathcal{T}}\cdot\nabla\psi_I dx. \tag{43}$$

We now analyze the first term in (43). Let f_p be the piecewise constant function such that on any $\tau\in\mathcal{T}$, $f_p = |\tau|^{-1}\int_\tau f(x)dx$, where $|\tau|$ is the area of the triangle τ. Therefore, by (40), Hölder's inequality, and the usual interpolation error estimates, we have

$$\begin{aligned} \int_\Omega f(\psi_I-\psi_{I'})dx &= \sum_{\tau\not\subset L_n}\int_\tau (f-f_p)(\psi_I-\psi_{I'})dx + \sum_{\tau\subset L_n}\int_\tau f(\psi_I-\psi_{I'})dx \\ &\le C\big(\sum_{\tau\not\subset L_n} h_\tau^2|f|_{H^1(\tau)}(|\psi|_{H^1(\tau)} + h_\tau|\psi|_{H^2(\tau)}) \\ &\qquad + \sum_{\tau\subset L_n}\|\rho f\|_{L^2(\tau)}\|\rho^{-1}(\psi_I-\psi_{I'})\|_{L^2(\tau)}\big). \end{aligned} \tag{44}$$

For a triangle $\tau\subset L_{i,j}$, $1\le i\le l$, $0\le j<n$, by (21), (13), (12), (15), (39), Proposition 3.4, and the fact $0<a_i\le 1$, we have

$$\begin{aligned} & h_\tau^2|f|_{H^1(\tau)}(|\psi|_{H^1(\tau)} + h_\tau|\psi|_{H^2(\tau)}) \\ &\qquad \le CN^{-1}\kappa_i^{2j}2^{2j}|f|_{H^1(\tau)}(|\psi|_{H^1(\tau)} + \kappa_i^j 2^{2j-2n}|\psi|_{H^2(\tau)}) \\ &\qquad \le CN^{-1}\|\rho^{2-c_i}\nabla f\|_{L^2(\tau)}(\|\rho^{-c_i}\nabla\psi\|_{L^2(\tau)} + 2^{2j-2n}\|\rho^{1-c_i}\nabla^2\psi\|_{L^2(\tau)}) \\ &\qquad \le CN^{-1}\|f\|_{\mathcal{K}^1_{\vec{a}-1}(\tau)}\|\psi\|_{\mathcal{K}^2_{\vec{a}+1}(\tau)}. \end{aligned} \tag{45}$$

For $\tau\subset\Omega_0 = \Omega\setminus\cup_i\mathbb{T}_{i,0}$, by $h_\tau\simeq N^{-1/2}$ and the equivalence between the H^m space and the $\mathcal{K}^m_\mu$ space, we have

$$h_\tau^2|f|_{H^1(\tau)}(|\psi|_{H^1(\tau)} + h_\tau|\psi|_{H^2(\tau)}) \le CN^{-1}\|f\|_{\mathcal{K}^1_{\vec{a}-1}(\tau)}\|\psi\|_{\mathcal{K}^2_{\vec{a}+1}(\tau)}. \tag{46}$$

For $\tau\subset L_{i,n}$, $1\le i\le l$, recall that τ is decomposed into three subregions G_j, $1\le j\le 3$, by its barycenter and midpoints of edges. On a subregion G_j that is away from the singular vertex v_i, since $G_j\cap\mathcal{V}=\emptyset$, by (13) and $\rho\simeq\kappa_i^n$, we have

$$\begin{aligned} \|\rho^{-1}(\psi_I-\psi_{I'})\|_{L^2(G_j)} &\le C\kappa_i^{-n}h_\tau(|\psi|_{H^1(G_j)} + h_\tau|\psi|_{H^2(G_j)}) \\ &\le CN^{-1/2}(\|\rho^{-c_i}\nabla\psi\|_{L^2(G_j)} + h_\tau\kappa_i^{-n}\|\rho^{1-c_i}\nabla^2\psi\|_{L^2(G_j)}) \\ &\le CN^{-1/2}\|\psi\|_{\mathcal{K}^2_{\vec{a}+1}(\tau)}. \end{aligned} \tag{47}$$

Now, let $G_j\subset\tau$ be the control volume associated with v_i. Let G be the union of all the control volumes in $\mathcal{T}'$ that are associated with the vertex v_i. Recall $\mathbb{T}_{i,n}$, the union of all triangles in $\mathcal{T}$ that have v_i has a vertex. Thus, it is clear that

$G_j \subset G \subset \mathbb{T}_{i,n}$. Since $\phi_I = 0$ on $\partial\Omega$, by the weighted Poincaré inequality [3, 31, 32] and (21), we have

$$\|\rho^{-1}\psi_I\|_{L^2(G)} \leq C|\psi_I|_{H^1(\mathbb{T}_{i,n})} \leq C(|\psi|_{H^1(\mathbb{T}_{i,n})} + N^{-1/2}\|\psi\|_{\mathcal{K}^2_{\vec{a}+1}(\mathbb{T}_{i,n})}),$$

where C is independent of n. Recall $\psi_{I'} = 0$ and $\rho \leq C\kappa_i^n$ on G. Therefore, by (12), we have

$$\begin{aligned}\|\rho^{-1}(\psi_I - \psi_{I'})\|_{L^2(G_j)} &\leq \|\rho^{-1}\psi_I\|_{L^2(G)} \leq C(|\psi|_{H^1(\mathbb{T}_{i,n})} + N^{-1/2}\|\psi\|_{\mathcal{K}^2_{\vec{a}+1}(\mathbb{T}_{i,n})}) \\ &\leq C\kappa_i^{nc_i}(\|\psi\|_{\kappa^1_{\vec{a}+1}(\mathbb{T}_{i,n})} + \kappa_i^{-nc_i}N^{-1/2}\|\psi\|_{\mathcal{K}^2_{\vec{a}+1}(\mathbb{T}_{i,n})}) \\ &\leq CN^{-1/2}\|\psi\|_{\mathcal{K}^2_{\vec{a}+1}(\mathbb{T}_{i,n})}. \qquad (48)\end{aligned}$$

Meanwhile for $\tau \subset L_{i,n}$, we have

$$\|\rho f\|_{L^2(\tau)} \leq \|f\|_{\mathcal{K}^1_{-1}(\tau)} \leq C\kappa_i^{nc_i}\|f\|_{\mathcal{K}^1_{\vec{a}-1}(\tau)} \leq CN^{-1/2}\|f\|_{\mathcal{K}^1_{\vec{a}-1}(\tau)}. \qquad (49)$$

Thus, by (44), (45), (46), (47), (48), (49), and the Cauchy-Schwarz inequality, we have

$$\begin{aligned}\int_\Omega f(\psi_I - \psi_{I'})dx \leq CN^{-1}\Big(&\sum_{\tau\not\subset L_n}\|f\|_{\mathcal{K}^1_{\vec{a}-1}(\tau)}\|\psi\|_{\mathcal{K}^2_{\vec{a}+1}(\tau)} \\ &+ \sum_{\tau\subset L_{i,n}, 1\leq i\leq l}\|f\|_{\mathcal{K}^1_{\vec{a}-1}(\tau)}\|\psi\|_{\mathcal{K}^2_{\vec{a}+1}(\mathbb{T}_{i,n})}\Big) \\ &\leq CN^{-1}\|f\|_{\mathcal{K}^1_{\vec{a}-1}(\Omega)}\|\psi\|_{\mathcal{K}^2_{\vec{a}+1}(\Omega)}. \qquad (50)\end{aligned}$$

Then, we analyze the last two terms in (43). Recall $\psi_{I'}$ is constant on each control volume and ψ_I is linear on each triangle. Then, by the Green formula and (41), we have

$$\begin{aligned}&-\sum_{E\in\mathcal{E}_{\mathcal{T}'}}\int_E \nabla u_{\mathcal{T}}\cdot\mathbf{n}_E[\psi_{I'}]ds - \int_\Omega \nabla u_{\mathcal{T}}\cdot\nabla\psi_I dx \\ &= \sum_{\tau\in\mathcal{T}}\int_{\partial\tau}\nabla u_{\mathcal{T}}\cdot\mathbf{n}\psi_{I'}ds - \sum_{\tau\in\mathcal{T}}\int_{\partial\tau}\nabla u_{\mathcal{T}}\cdot\mathbf{n}\psi_I ds \\ &= \sum_{\tau\in\mathcal{T}}\int_{\partial\tau}\nabla u_{\mathcal{T}}\cdot\mathbf{n}(\psi_{I'} - \psi_I)ds = 0. \qquad (51)\end{aligned}$$

Thus, by (42), (43), (50), (51), Theorem 3.6, Proposition 3.4, Theorem 3.9, and the Cauchy-Schwarz inequality, we have

$$\begin{aligned}\|u - u_{\mathcal{T}}\|^2_{L^2(\Omega)} &\leq C\|\psi - \psi_I\|_{H^1(\Omega)}\|u - u_{\mathcal{T}}\|_{H^1(\Omega)} \\ &\quad + CN^{-1}\|f\|_{\mathcal{K}^1_{\vec{a}-1}(\Omega)}\|u - u_{\mathcal{T}}\|_{\mathcal{K}^0_{\vec{a}-1}(\Omega)} \\ &\leq CN^{-1}\|u - u_{\mathcal{T}}\|_{\mathcal{K}^0_{\vec{a}-1}(\Omega)}\|f\|_{\mathcal{K}^0_{\vec{a}-1}(\Omega)} + CN^{-1}\|f\|_{\mathcal{K}^1_{\vec{a}-1}(\Omega)}\|u - u_{\mathcal{T}}\|_{\mathcal{K}^0_{\vec{a}-1}(\Omega)} \\ &\leq CN^{-1}\|f\|_{\mathcal{K}^1_{\vec{a}-1}(\Omega)}\|u - u_{\mathcal{T}}\|_{L^2(\Omega)}.\end{aligned}$$

This completes the proof. □

Remark 3.12. The estimates in Theorem 3.9 and Corollary 3.11 hold as long as the given function f is in the specified weighted space. In particular, for $0 < a_i \leq 1$, $H^1(\Omega) \subset \mathcal{K}^1_{\vec{a}-1}(\Omega)$. Therefore, the L^2 error analysis in Corollary 3.11 holds for any $f \in H^1(\Omega)$.

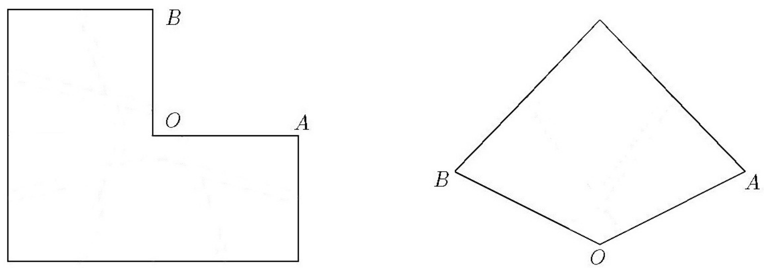

FIGURE 5. Two computational domains: the L-shaped domain for the first test set (left) and the quadrilateral domain for the second test set (right).

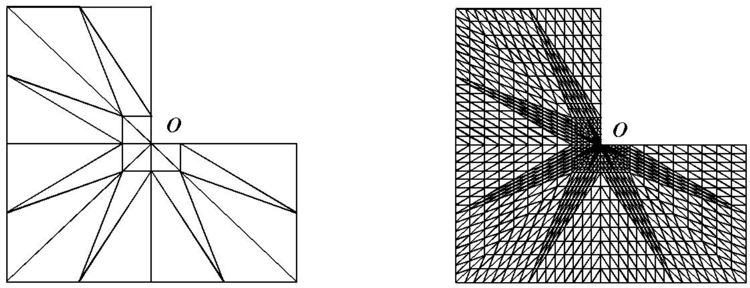

FIGURE 6. Graded meshes on the L-shaped domain for linear FVMs: $\mathcal{T}_0$ (left) and $\mathcal{T}_3$ (right), $\vec{\kappa} = (0.2, 0.5, 0.5, 0.5, 0.5, 0.5)$.

4. Numerical tests

We consider the following elliptic equation

$$-\triangle u = f \quad \text{in} \quad \Omega, \qquad u = g \quad \text{on} \quad \partial\Omega \tag{52}$$

on two polygonal domains (Figure 5): the L-shaped domain ($\angle AOB = 3\pi/2$) and the quadrilateral domain ($\angle AOB = 2\pi/3$). In the tests below, we always let the vertex O be the first vertex of the domain, namely, $v_1 = O$.

TABLE 1. H^1-norm of the errors: the linear FVMs on the L-shaped domain.

j	$\lvert u - u_j \rvert_{H^1(\Omega)}$				
	κ_1=0.1	κ_1=0.2	κ_1=0.3	κ_1=0.4	κ_1=0.5
1	1.46E-01(0.93)	1.21E-01(0.98)	1.13E-01(0.98)	1.19E-01(0.91)	1.37E-01(0.77)
2	8.15E-02(0.94)	6.59E-02(0.97)	6.26E-02(0.95)	7.00E-02(0.86)	8.83E-02(0.71)
3	4.32E-02(0.97)	3.45E-02(0.98)	3.37E-02(0.94)	4.03E-02(0.84)	5.64E-02(0.68)
4	2.22E-02(0.98)	1.77E-02(0.99)	1.77E-02(0.95)	2.29E-02(0.83)	3.59E-02(0.67)
5	1.12E-02(0.99)	8.97E-03(0.99)	9.24E-03(0.95)	1.29E-02(0.84)	2.27E-02(0.66)
6	5.64E-03(1.00)	4.51E-03(0.99)	4.76E-03(0.96)	7.21E-03(0.84)	1.43E-02(0.66)
7	2.82E-03(1.00)	2.26E-03(0.99)	2.43E-03(0.97)	4.01E-03(0.85)	9.08E-03(0.66)

4.1. Linear FVMs. In the first set of tests, we solve equation (52) on the L-shaped domain (Figure 5) using the linear FVMs associated with the barycenter

TABLE 2. L^2-norm of the errors: the linear FVM on the L-shaped domain.

j	$\|u-u_j\|_{L^2(\Omega)}$				
	κ_1=0.1	κ_1=0.2	κ_1=0.3	κ_1=0.4	κ_1=0.5
1	2.51E-02(1.84)	1.61E-02(1.93)	1.29E-02(1.95)	1.41E-02(1.87)	1.98E-02(1.60)
2	7.70E-03(1.90)	4.70E-03(1.99)	3.85E-03(1.95)	4.65E-03(1.78)	7.81E-03(1.50)
3	2.14E-03(1.95)	1.27E-03(2.00)	1.08E-03(1.94)	1.49E-03(1.74)	3.05E-03(1.43)
4	5.63E-04(1.98)	3.29E-04(2.00)	2.93E-04(1.93)	4.68E-04(1.72)	1.19E-03(1.39)
5	1.43E-04(2.00)	8.37E-05(2.00)	7.79E-05(1.94)	1.45E-04(1.71)	4.66E-04(1.37)
6	3.61E-05(2.00)	2.11E-05(2.00)	2.04E-05(1.94)	4.46E-05(1.71)	1.82E-04(1.36)
7	9.05E-06(2.00)	5.28E-06(2.00)	5.29E-06(1.95)	1.36E-05(1.71)	7.18E-05(1.35)

dual mesh (Definition 2.1). We assign the exact solution

$$u = r^{\frac{2}{3}} \sin(\frac{2}{3}(\theta - \frac{\pi}{2})),$$

where (r, θ) is the polar coordinate at the origin $O = (0, 0)$, and f and g are obtained from the equation and u. This solution has a typical corner singularity near the reentrant corner at O: $u \in H^{\frac{5}{3}-\epsilon}(\Omega) \notin H^2(\Omega)$ for any $\epsilon > 0$, and therefore the linear FVM can not achieve the optimal convergence rate on a quasi-uniform mesh. We implement the linear FVM on graded meshes with different grading parameters toward the vertex $O = v_1$. See Figure 6 for an example of the mesh refinements. The H^1-norm and L^2-norm of the errors are presented in Table 1 and Table 2. Next to the error, displayed in the parentheses is the error reduction rate that is calculated by

$$\log_2(\frac{\|u - u_{j-1}\|}{\|u - u_j\|}), \tag{53}$$

where u_j is the FV solution on the mesh obtained after j refinements, and the norm is either H^1 or L^2, depending on the type of convergence rate we focus on. In this example, we have a singular corner at O with angle $\phi_1 = 3\pi/2$, while the solution $u \in H^2$ on any subregion that is away from the first vertex O. Therefore, according to Theorem 3.9 and Corollary 3.11, we should choose the grading parameter

$$0 < \kappa_1 < 2^{-3/2} \approx 0.354 \tag{54}$$

and it is sufficient to use quasi-uniform meshes ($\kappa_i = 0.5$) near other corners of the domain, in order to obtain the optimal convergence rates in the H^1 and L^2 norms. In the tests, we report the error reduction rates on meshes with $\kappa_i = 0.5$, $i = 2, 3, 4, 5, 6$, but for different values of κ_1. It is shown in Table 1 and Table 2 that the H^1 and L^2 error reduction rates are optimal (i.e., 1 and 2), respectively, for $\kappa_1 = 0.1, 0.2, 0.3$; while for $\kappa_1 = 0.4, 0.5$, the convergence rates deviate from the optimal orders. This convergence behavior clearly verifies our theory that predicts the optimal range (54) for the grading parameter.

4.2. Quadratic element. In the second set of tests, using quadratic FVMs, we solve equation (52) on the quadrilateral domain with vertices $(0, 0)$, $(1, \frac{1}{\sqrt{3}})$, $(-1, \frac{1}{\sqrt{3}})$, and $(0, \frac{1}{\sqrt{3}} + \cot(\frac{2}{9}\pi))$ (Figure 5). We assign the exact solution

$$u = r^{\frac{3}{2}} \sin(\frac{3}{2}(\theta - \frac{\pi}{6})),$$

and obtain f and g from the equation and u. The quadratic FVM is constructed with respect to the dual mesh with $\alpha = \beta = 1/3$ (Definition 2.2). This solution

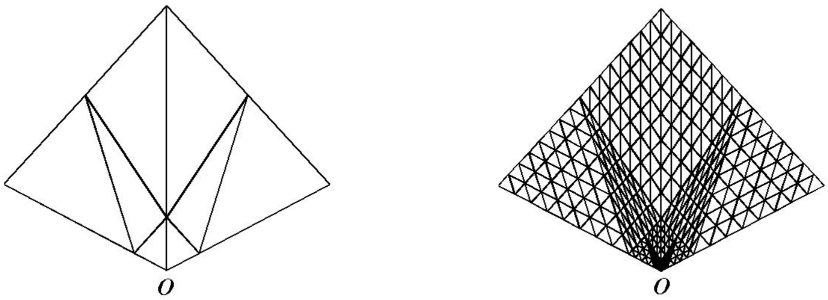

FIGURE 7. Graded meshes on the quadrilateral domain for quadratic FVMs: $\mathcal{T}_0$ (left) and $\mathcal{T}_3$ (right), $\vec{\kappa} = (0.2, 0.5, 0.5, 0.5)$.

TABLE 3. H^1-norm of the errors: the quadratic FVMs on the quadrilateral domain.

j	$\|u-u_j\|_{H^1(\Omega)}$				
	κ_1=0.1	κ_1=0.2	κ_1=0.3	κ_1=0.4	κ_1=0.5
1	3.66E-02(1.01)	2.51E-02(1.74)	1.93E-02(2.26)	1.93E-02(2.26)	2.35E-02(1.87)
2	1.15E-02(1.95)	7.50E-03(2.05)	5.57E-03(2.11)	5.75E-03(2.06)	8.63E-03(1.71)
3	3.36E-03(1.94)	2.03E-03(2.05)	1.50E-03(2.06)	1.65E-03(1.96)	3.10E-03(1.61)
4	9.05E-04(1.98)	5.25E-04(2.04)	3.89E-04(2.03)	4.60E-04(1.92)	1.10E-03(1.55)
5	2.33E-04(2.00)	1.33E-04(2.02)	9.91E-05(2.01)	1.26E-04(1.90)	3.92E-04(1.52)
6	5.89E-05(2.00)	3.34E-05(2.01)	2.49E-05(2.01)	3.42E-05(1.90)	1.38E-04(1.51)

has a corner singularity at O: $u \in H^{\frac{5}{2}-\epsilon}(\Omega) \notin H^3(\Omega)$ for $\epsilon > 0$, and therefore the quadratic FVM can not get the optimal convergence rate on quasi-uniform meshes. Note that the solution is in H^3 except for the neighborhood of the vertex $v_1 = O$. Thus, we shall choose quasi-uniform meshes near other corners ($\kappa_i = 0.5$, $i = 2, 3, 4$) in the tests. Appropriate mesh grading near O, however, is necessary to improve the convergence of the numerical solution.

In this example, we have a singular corner at O with $\phi_1 = 2\pi/3$. Therefore, according to Theorem 3.9, we should choose the grading parameter

$$0 < \kappa_1 < 2^{-4/3} \approx 0.397 \tag{55}$$

to obtain the optimal convergence rate for the quadratic FVM. See Figure 7 for an example of the graded mesh refinement. The H^1-norm of the errors and the convergence orders (53) are presented in Table 3. It is clear that the H^1-norm error reduction rates are 2 for $\kappa_1 = 0.1, 0.2, 0.3$; while for $\kappa_1 = 0.4, 0.5$, the convergence rates deviate from the optimal orders. This again confirms our construction (55) of optimal quadratic FVMs for singular solutions.

References

[1] T. Apel, A.-M. Sändig, and J. Whiteman. Graded mesh refinement and error estimates for finite element solutions of elliptic boundary value problems in non-smooth domains. Math. Methods Appl. Sci., 19(1):63–85, 1996.

[2] I. Babuška, R. Kellogg, and J. Pitkäranta. Direct and inverse error estimates for finite elements with mesh refinements. Numer. Math., 33(4):447–471, 1979.

[3] C. Băcuţă, V. Nistor, and L. T. Zikatanov. Improving the rate of convergence of 'high order finite elements' on polygons and domains with cusps. Numer. Math., 100(2):165–184, 2005.

[4] R. E. Bank and D. J. Rose. Some error estimates for the box method. SIAM J. Numer. Anal., 24(4):777–787, 1987.

[5] T. Barth and M. Ohlberger. Finite volume methods: foundation and analysis. Lecture Notes in Mathematics, Vol. 268. John Wiley & Sons, 2004. Encyclopedia of computational Mechanics, volume 1, chapter 15.

[6] Z. Cai, J. Douglas, Jr., and M. Park. Development and analysis of higher order finite volume methods over rectangles for elliptic equations. Adv. Comput. Math., 19(1-3):3–33, 2003. Challenges in computational mathematics (Pohang, 2001).

[7] Z. Q. Cai. On the finite volume element method. Numer. Math., 58(7):713–735, 1991.

[8] W. Cao, Z. Zhang, and Q. Zou. Superconvergence of any order finite volume schemes for 1D general elliptic equations. J. Sci. Comput., 56(3):566–590, 2013.

[9] P. Chatzipantelidis and R. D. Lazarov. Error estimates for a finite volume element method for elliptic PDEs in nonconvex polygonal domains. SIAM J. Numer. Anal., 42(5):1932–1958, 2005.

[10] Z. Chen, R. Li, and A. Zhou. A note on the optimal L^2-estimate of the finite volume element method. Adv. Comput. Math., 16(4):291–303, 2002.

[11] Z. Chen, J. Wu, and Y. Xu. Higher-order finite volume methods for elliptic boundary value problems. Adv. Comput. Math., 37(2):191–253, 2012.

[12] Z. Chen, Y. Xu, and Y. Zhang. A construction of higher-order finite volume methods. Math. Comp., 84(292):599–628, 2015.

[13] M. Costabel, M. Dauge, and S. Nicaise. Analytic regularity for linear elliptic systems in polygons and polyhedra. Math. Models Methods Appl. Sci., 22(8):1250015, 63, 2012.

[14] M. Dauge. Elliptic Boundary Value Problems on Corner Domains, volume 1341 of Lecture Notes in Mathematics. Springer-Verlag, Berlin, 1988.

[15] K. Djadel, S. Nicaise, and J. Tabka. Some refined finite volume methods for elliptic problems with corner singularities. Int. J. Finite Vol., 1(1):33, 2004.

[16] P. Emonot. Methods de volums elements finis : applications aux equations de navier-stokes et resultats de convergence. Lyon, 1992. Dissertation.

[17] L. Evans. Partial differential equations, volume 19 of Graduate Studies in Mathematics. AMS, Rhode Island, 1998.

[18] R. E. Ewing, T. Lin, and Y. Lin. On the accuracy of the finite volume element method based on piecewise linear polynomials. SIAM J. Numer. Anal., 39(6):1865–1888, 2002.

[19] R. Eymard, T. Gallouët, and R. Herbin. Finite volume methods. In Handbook of numerical analysis, Vol. VII, Handb. Numer. Anal., VII, pages 713–1020. North-Holland, Amsterdam, 2000.

[20] D. Gilbarg and N. S. Trudinger. Elliptic partial differential equations of second order. Classics in Mathematics. Springer-Verlag, Berlin, 2001. Reprint of the 1998 edition.

[21] P. Grisvard. Singularities in boundary value problems, volume 22 of Research Notes in Applied Mathematics. Springer-Verlag, New York, 1992.

[22] B. Guo and C. Schwab. Analytic regularity of Stokes flow on polygonal domains in countably weighted Sobolev spaces. J. Comput. Appl. Math., 190(1-2):487–519, 2006.

[23] W. Hackbusch. On first and second order box schemes. Computing, 41(4):277–296, 1989.

[24] B. Heinrich. Finite difference methods on irregular networks, volume 82 of Internationale Schriftenreihe zur Numerischen Mathematik [International Series of Numerical Mathematics]. Birkhäuser Verlag, Basel, 1987. A generalized approach to second order elliptic problems.

[25] J. M. Hyman, R. J. Knapp, and J. C. Scovel. High order finite volume approximations of differential operators on nonuniform grids. Phys. D, 60(1-4):112–138, 1992. Experimental mathematics: computational issues in nonlinear science (Los Alamos, NM, 1991).

[26] V. A. Kondrat′ev. Boundary value problems for elliptic equations in domains with conical or angular points. Trudy Moskov. Mat. Obšč., 16:209–292, 1967.

[27] V. Kozlov, V. Maz'ya, and J. Rossmann. Spectral problems associated with corner singularities of solutions to elliptic equations, volume 85 of Mathematical Surveys and Monographs. American Mathematical Society, Providence, RI, 2001.

[28] R. D. Lazarov, I. D. Mishev, and P. S. Vassilevski. Finite volume methods for convection-diffusion problems. SIAM J. Numer. Anal., 33(1):31–55, 1996.

[29] Y.-J. Lee and H. Li. Axisymmetric Stokes equations in polygonal domains: Regularity and finite element approximations. Comput. Math. Appl., 64(11):3500–3521, 2012.

[30] R. J. LeVeque. Finite volume methods for hyperbolic problems. Cambridge Texts in Applied Mathematics. Cambridge University Press, Cambridge, 2002.
[31] H. Li. Finite element analysis for the axisymmetric Laplace operator on polygonal domains. J. Comput. Appl. Math., 235:5155–5176, 2011.
[32] H. Li. Regularity and multigrid analysis for Laplace-type axisymmetric equations. Math. Comp., 84:1113–1144, 2015.
[33] H. Li, A. Mazzucato, and V. Nistor. Analysis of the finite element method for transmission/mixed boundary value problems on general polygonal domains. Electron. Trans. Numer. Anal., 37:41–69, 2010.
[34] R. Li, Z. Chen, and W. Wu. Generalized Difference Methods for Partial Differential Equations. Chapman & Hall/CRC Pure and Applied Mathematics. McGraw Hill, New York, 1980.
[35] F. Liebau. The finite volume element method with quadratic basis functions. Computing, 57(4):281–299, 1996.
[36] J.-L. Lions and E. Magenes. Non-homogeneous boundary value problems and applications. Vol. I. Springer-Verlag, New York-Heidelberg, 1972. Translated from the French by P. Kenneth, Die Grundlehren der mathematischen Wissenschaften, Band 181.
[37] R. H. Macneal. An asymmetrical finite difference network. Quart. Math. Appl., 11:295–310, 1953.
[38] P. Morin, R. Nochetto, and K. Siebert. Convergence of adaptive finite element methods. SIAM Rev., 44(4):631–658 (electronic) (2003), 2002. Revised reprint of "Data oscillation and convergence of adaptive FEM" [SIAM J. Numer. Anal. **38** (2000), no. 2, 466–488 (electronic); MR1770058 (2001g:65157)].
[39] R. A. Nicolaides, T. A. Porsching, and C. A. Hall. L_∞-convergence of finite element approximations. pages 279–299. Computational Fluid Dynamics Review. Wiley, New York,, 1995.
[40] C. Ollivier-Goocha and M. V. Altena. A high-order-accurate unstructured mesh finite-volume scheme for the advection diffusion equation. J. Comput. Phys., 181:729–752, 2002.
[41] S. V. Patanker. Numerical Heat Transfer and Fluid Flow. Ser. Comput. Methods Mech. Thermal Sci. CRC Press, 2000.
[42] M. Plexousakis and G. E. Zouraris. On the construction and analysis of high order locally conservative finite volume-type methods for one-dimensional elliptic problems. SIAM J. Numer. Anal., 42(3):1226–1260 (electronic), 2004.
[43] G. Raugel. Résolution numérique par une méthode d'éléments finis du problème de Dirichlet pour le laplacien dans un polygone. C. R. Acad. Sci. Paris Sér. A-B, 286(18):A791–A794, 1978.
[44] C.-W. Shu. High-order finite difference and finite volume WENO schemes and discontinuous Galerkin methods for CFD. Int. J. Comput. Fluid Dyn., 17(2):107–118, 2003.
[45] J. Xu and Q. Zou. Analysis of linear and quadratic simplicial finite volume methods for elliptic equations. Numer. Math., 111(3):469–492, 2009.
[46] Z. Zhang and Q. Zou. A family of finite volume schemes of arbitrary order on rectangular meshes. J. Sci. Comput., 58(2):308–330, 2014.

Guanghao Jin, Endo Lab, Tokyo Institute of Technology, Tokyo, 1528552, Japan
E-mail: `jin.g.ab@m.titech.ac.jp`

Hengguang Li, Department of Mathematics, Wayne State University, Detroit, MI 48202, USA
E-mail: `hli@math.wayne.edu`

Qinghui Zhang, Guangdong Province Key Laboratory of Computational Science and School of Data and Computer Science, Sun Yat-Sen University, Guangzhou, 510275, P. R. China
E-mail: `zhangqh6@mail.sysu.edu.cn`

School of Data and Computer Science and Guangdong Province Key Laboratory of Computational Science, Sun Yat-sen University, Guangzhou 510275, P. R. China
E-mail: `mcszqs@mail.sysu.edu.cn`